



GLOBAL JOURNAL OF SCIENCE FRONTIER RESEARCH: A
PHYSICS AND SPACE SCIENCE
Volume 15 Issue 1 Version 1.0 Year 2015
Type : Double Blind Peer Reviewed International Research Journal
Publisher: Global Journals Inc. (USA)
Online ISSN: 2249-4626 & Print ISSN: 0975-5896

Is Spacetime Fractal and Quantum Coherent in the Golden Mean?

By Mae-Wan Ho, Mohamed el Naschie & Giuseppe Vitiello

University of Salerno, Italy

Abstract- We consider the fabric of spacetime from a wide perspective: from mathematics, quantum physics, far from equilibrium thermodynamics, biology and neurobiology. It appears likely that spacetime is fractal and quantum coherent in the golden mean. Mathematically, our fractal universe is non-differentiable and discontinuous, yet dense in the infinite dimensional spacetime. Physically, it appears to be a quantum coherent universe consisting of an infinite diversity of autonomous agents all participating in co-creating organic, fractal spacetime by their multitudinous coupled cycles of activities. Biologically, this fractal coherent spacetime is also the fabric of conscious awareness mirrored in the quantum coherent golden mean brain states.

Keywords: *whitehead's philosophy, discontinuous nondifferentiable spacetime, fractals, coupled activity cycles, deterministic chaos, quantum coherence and fractals, golden mean.*

GJSFR-A Classification : *FOR Code: 020699, 020109*



Strictly as per the compliance and regulations of :



Is Spacetime Fractal and Quantum Coherent in the Golden Mean?

Mae-Wan Ho^α, Mohamed el Naschie^σ & Giuseppe Vitiello^ρ

Abstract- We consider the fabric of spacetime from a wide perspective: from mathematics, quantum physics, far from equilibrium thermodynamics, biology and neurobiology. It appears likely that spacetime is fractal and quantum coherent in the golden mean. Mathematically, our fractal universe is non-differentiable and discontinuous, yet dense in the infinite dimensional spacetime. Physically, it appears to be a quantum coherent universe consisting of an infinite diversity of autonomous agents all participating in co-creating organic, fractal spacetime by their multitudinous coupled cycles of activities. Biologically, this fractal coherent spacetime is also the fabric of conscious awareness mirrored in the quantum coherent golden mean brain states.

Keywords: *Whitehead's philosophy, discontinuous nondifferentiable spacetime, fractals, coupled activity cycles, deterministic chaos, quantum coherence and fractals, golden mean.*

I. INTRODUCTION

Is spacetime fractal and quantum coherent in the golden mean? This is too deep and fundamental a question to be answered definitively on the basis of our present knowledge. However, one could try to get a good idea on the properties of spacetime in a number of mathematical and physical features emerging from research activities in many fields, including mathematics, quantum physics, far from equilibrium thermodynamics, biology and neurobiology, which also hark back to some basic problems in philosophy. Our attempt in this paper is to bring together the relevant observations and findings without claiming to be complete, that support our speculation concerning the basic “fabric” of spacetime. In so doing, we connect the ubiquitous recurrence of the golden mean and fractal self-similarity in microscopic and macroscopic phenomena with the coherent state dynamics at the quantum level and effects at the macroscopic level.

We start with the nature of the spacetime as perceived by Alfred North Whitehead (1861-1947) and others.

II. REAL PROCESSES DO NOT HAPPEN AT POINTS IN A SPACETIME CONTINUUM

As one of us (MWH) has commented [1], Whitehead lived through an exciting era in Western

science when the fabric of physical reality - Newton's flat, smooth, and static absolute spacetime - was being thoroughly ruffled by Albert Einstein's theories of special and general relativity and by quantum mechanics. The modern observer no longer views nature from the outside, being irreducibly quantum-entangled with the known, possibly with all entities in the entire universe.

These surprising lessons from nature became the basis of Whitehead's perennial philosophy (a cosmogony) [2], ushering in a new age of the organism that inspired generations of scientists. He saw the universe as a super-organism encompassing organisms on every scale from galaxies to elementary particles, and argued it is only possible to know and understand nature both as an organism and with the sensitivity of an organism.

Most important, though least understood was his rejection of the mechanical laws of classical physics and differential calculus for their failure to describe real processes. Not only do they leave out of account the all-important knowing experiencing organism, real processes occur in *intervals* of time associated with volumes of space. Absolutely nothing can happen at a point in an instant.

Rather than a smooth, infinitely divisible continuum, spacetime is more likely discrete and discontinuous, and hence *non-differentiable*, as quantum physics has already discovered at the smallest scale. Unfortunately, mathematics had lagged behind physics. Both relativity theory and quantum theory inherited the predominant mathematics of classical mechanics.

Roger Penrose's *The Road to Reality, A Complete Guide to the Laws of The Universe* [3] charts the heroic and ingenious efforts of mathematical physicists to grasp hold of post Newtonian universe, which in the end they failed to do. The dream of uniting the two great theories of quantum physics and general relativity has remained unfulfilled; not least because these two modern theories are both based on the foundation of classical physics: a differentiable, continuous, spacetime manifold.

The issue of continuity versus discontinuity of spacetime did not originate in Newtonian mechanics. It can be traced back to ancient Greek philosophy, especially in Zeno's paradox of Achilles and the tortoise [4] (see Appendix 1). It is generally thought that Newton and Leibniz had both resolved Zeno's paradox with

Author α: *Institute of Science in Society, Edge Institute International, London UK and Italy. e-mail: m.w.ho@i-sis.org.uk.*

Author σ: *Alexandria University, Egypt.*

Author ρ: *University of Salerno, Edge Institute International, London UK and Italy.*

differential calculus, by inventing infinitesimal space and time intervals. Whitehead [2] and Henri Bergson [5] were among those who would not have accepted this 'resolution'.

Zeno's paradox was about the impossibility of motion as represented by an infinite sequence of static configurations of matter at points in time. Whitehead said in his *Concept of Nature* ([6] p. 15): "There is no holding nature still and looking at it." The absolute, infinitely divisible time and space of Newtonian physics are both abstractions from ever owing events of nature. He concurred with Bergson [5] in using the concept of 'duration' ([6], p. 53) for an interval of time experienced by the knower as a simultaneity encompassing 'a complex of partial events'. We shall show later that 'duration' and 'simultaneity' can be given very specific meanings in terms of characteristic time of processes and coherence time.

III. MATHEMATICS OF DISCONTINUITY

The Cantor set, discovered by Georg Cantor in 1883 [7], is fundamental for discontinuous mathematics. Its apparently paradoxical nature is that it is infinitely sub-divisible, but is completely discontinuous and nowhere dense. It is also a fractal with self-similar patterns on every scale [8].

The mathematics of non-differentiable and discontinuous spaces is among the most significant discoveries/inventions beginning with Cantor in the late 19th century, though it did not really take off until well into the 20th century, reaching its peak in the science and mathematics of complexity associated especially with Benoit Mandelbrot's fractals [9] and Edward Lorenz' deterministic chaos [10],[11].

We provide informal definitions of some mathematical terms that will be used in this paper in Appendix 2 (from [1]); some, like deterministic chaos, have no generally agreed definition.

IV. CONTINUOUS NON-DIFFERENTIABLE FRACTAL SPACETIME

Garnet Ord was the first to propose a fractal spacetime and to coin the term for it [12]. His starting point was Richard Feynman's observation [13] that when they are looked at on a sufficiently fine scale, the paths of quantum mechanical particles are non-differentiable curves rather than straight lines. Moreover, relativistic interaction with particles at sufficiently high energies produces non-conserved particle numbers. These and other anomalies have encouraged quantum mechanics to abandon the concept of a point particle and its trajectory in favour of wavepackets or field excitations. Feynman's formulation in terms of path integrals was an exception. In the same spirit, Ord set out to construct a continuous trajectory in spacetime that exhibits features analogous to those in relativistic

quantum mechanics. He came up with a fractal trajectory exemplified by a Peano-Moore curve (Figure 1). It is plane-filling with a fractal (Hausdorff) dimension of 2 instead of the classical linear path that has a dimension of 1.

Ord showed that, among other things, such a fractal trajectory exhibits both an uncertainty principle and a de Broglie relation. On a microscopic scale, the presence of fractal time is interpreted in terms of the appearance of particle-antiparticle pairs when observation energies are of the order of mc^2 . On a macroscopic scale greater than the fractal wavelength, the free 'fractalons' appear to move on a classical one-dimensional trajectory.

A more elaborate scale-relativity theory of fractal spacetime was proposed by Laurent Nottale [14], who was motivated by "the failure of a large number of attempts to understand the quantum behavior in terms of standard differentiable geometry" to look for a possible "quantum geometry", i.e., fractals [15], (pp.4-5). His theory recovers quantum mechanics as mechanics on a nondifferentiable spacetime, and the Schrödinger equation is demonstrated as a geodesic equation.

Ord and Nottale have both proposed fractal spacetimes that are continuous and nondifferentiable.

A more radical cosmology proposed by one of us (MeN) is a fractal spacetime that is based on the golden mean and is neither continuous nor differentiable (see below). It is closest to our intuitive notion of organic (as opposed to mechanical) spacetime, and more intimately connected to our emerging understanding of biological spacetime [1].

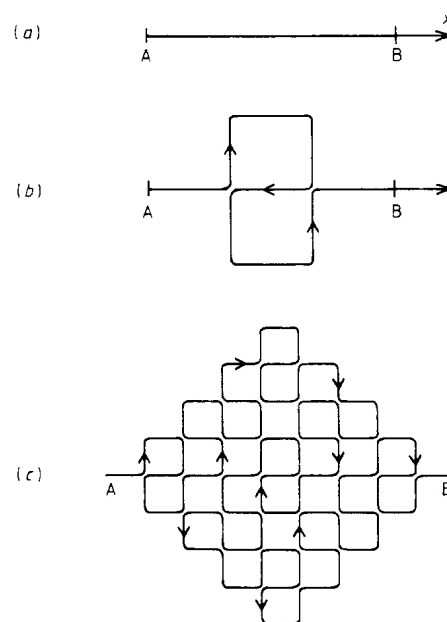


Figure 1 : A particle's fractal trajectory at increasing resolution, at scale (a): $s = \lambda$, (b): $s = \lambda/3$, (c): $s = \lambda/9$. (from [13])

V. \mathcal{E}^∞ SPACETIME AND OUR 4-DIMENSIONAL UNIVERSE

MeN's work was first reviewed by MWH [1], who provided a simplified account that we recapitulate here.

\mathcal{E}^∞ (E-infinity) is an infinite dimensional fractal spacetime. Yet its Hausdorff dimension is 4.236067977... This means that at ordinary scales, it looks and feels 4 dimensional (three of space and one of time), with the remaining dimensions 'compacted' in the remaining 0.236067977 "fuzzy tail" [16]. One imagine such a universe as a four dimensional hypercube with further four dimensional hypercubes

nested inside like Russian dolls [17] (see figure 2). The exact Hausdorff dimension of the infinite dimensional hypercube is $4+\phi^3$, where $\phi = (\sqrt{5}-1)/2$, the golden mean. The dimension $4+\phi^3$ can be expressed as the following self-similar continued fraction which converges to precisely $4+\phi^3$:

$$4 + \phi^3 = 4 + \frac{1}{4 + \frac{1}{4 + \frac{1}{4 + \frac{1}{4 + \dots}}}}$$

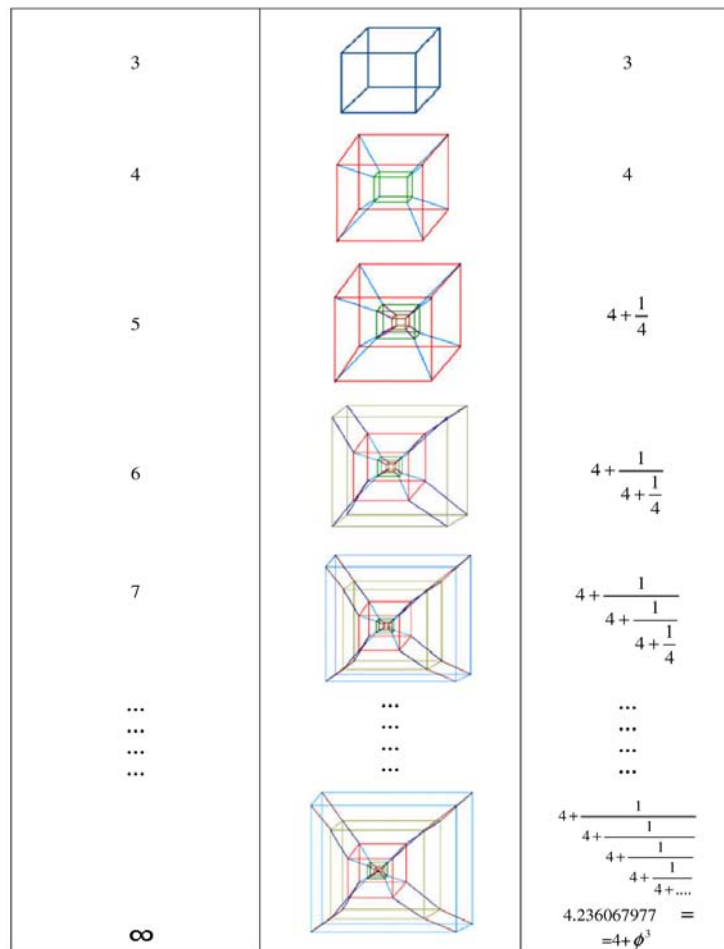


Figure 2 : A Euclidean representation of [einfinity-spacetime] \mathcal{E}^∞ fractal spacetime as an infinite sequence of nested four dimensional hypercubes (redrawn from [16])

The 4-dimensional hypercube is the Euclidean representation of the E-infinity universe. It is a challenge to represent \mathcal{E}^∞ in its proper non-Euclidean form.

Another mathematical property of the Cantor set is that its cardinality (number of points or elements) is exactly the same as the original continuous line. Thus, the Cantor set is a perfect compromise between the discrete and the continuum; it is a discrete structure that has the same number of elements as the continuum.

Mathematically, the \mathcal{E}^∞ universe is a random Cantor set extended to infinite dimensions. Remarkably, the Hausdorff dimension of this infinite extension is no larger than $4+\phi^3$.

Figure 3 illustrates the steps involved in deriving \mathcal{E}^∞ universe. Recall that the standard Cantor set is obtained by dividing the unit interval into three parts and removing the middle part, leaving the end points. Then do the same to each of the two remaining parts. We

repeat the process infinitely often, and in the end there remain only isolated points, or 'Cantor dust'. The Menger-Urysohn dimension is 0, but the Hausdorff dimension is $\log 2 / \log 3$.

If however at each step we remove not necessarily the middle section but any one of the three

chosen at random, then again we are left with isolated points but now the Hausdorff dimension is the golden mean $\phi = (\sqrt{5} - 1)/2 = 0.61803398 \dots$. This Important result, proven by Mauldin and Williams in 1986 [18], is what makes it possible to derive the \mathcal{E}^∞ universe with all its remarkable properties, as we shall see.









Type of fractal	Geometrical shape	Menger-Urysohn dimension	Hausdorff dimension	Corresponding random Hausdorff dimension	Embedding dimension	Corresponding Euclidean shape
Cantor Set		0	$\ln 2 / \ln 3 = 0.630929753$	$\phi = 0.61803398$	1	 Line
Sierpinski gasket		2	$\ln 3 / \ln 2 = 1.584962501$	$\frac{1}{\phi} = 1.618033989$	2	 Square
Menger sponge		3	$D_{MS} = \ln 20 / \ln 3 = 2.7268$	$2 + \phi = 2.61803398$	3	 Cube
The 4 dimension random cantor set analogue of Menger sponge	 <i>An artist impression of $\mathcal{E}^{(4)}$ space-time</i>	4	$d_c^{(4)} = 4.236068$	$4 + \phi^3 = 4.23606797$	5	 Hyper cube

Figure 3: Fractals and dimensions in the derivation of E infinity spacetime

We now construct the higher dimensional random Cantor spaces [16] (see Fig. 3). The 2-dimensional version is the Sierpinski gasket, with Hausdorff dimension of $1/\phi \approx 1.61803398$; the 3-dimensional version is the Menger sponge, with Hausdorff dimension $2 + \phi \approx 2.61803398$. These are both well-known geometric shapes. The 4-dimensional version, with Hausdorff dimension $4 + \phi^3 \approx 4.2360679$, is given only an artist's representation. The 4-dimensional version is the same as the \mathcal{E}^∞ universe constructed from an infinite number of random Cantor sets, as will be made clear later. Note that the diagram representing the 4-dimensional Cantorian spacetime is space-filling with smaller and smaller spheres. This space-filling property makes the Cantorian spacetime non-differentiable and discontinuous, yet dense everywhere in spacetime. It recalls the quasi-periodic Penrose tiling in 2 dimensions of Euclidean (flat) space where the golden mean is key (see [19] and references therein). Branching processes based on the golden mean are also space-filling [20], as

are spiral leave arrangement patterns with the golden angle between successive leaf primordial (see [21]).

MeN has presented several different formal derivations of \mathcal{E}^∞ spacetime; we give here the simplest [16],[17] which is based on the mathematical properties of Borel sets to which Cantor sets belong.

The expectation value of the Hausdorff dimension of the Cantor set extended to infinity is simply a sum over n , for $n = 0$ to $n = \infty$, of n multiplied by the Hausdorff dimension of the random Cantor set raised to the power n .

$$\langle \text{Dim} E - \infty \rangle = \sum_0^\infty n (d_c^{(0)})^n \quad (1)$$

where the superscript in $d_c^{(0)}$ refers to the Menger-Urysohn dimension of the random Cantor set, which is 0, while the corresponding Hausdorff dimension $d_c^{(0)}$ is ϕ . Summing up the infinite number of terms gives the answer $4 + \phi^3$ exactly, as follows:

$$\begin{aligned} \langle \text{Dim} E - \infty \rangle &= (0) + (1)(\phi)^1 + (2)(\phi)^2 + (3)(\phi)^3 + \dots \\ &= 4 + \phi^3 \\ &= 4.236067977 \dots \end{aligned} \quad (2)$$

The intersection rule of sets, the 'bijection formula', relates the Menger-Urysohn dimension to the Hausdorff dimension. It shows that we can lift $d_c^{(0)}$ to

$$d_c^{(n)} = (1/d_c^{(0)})^{n-1} \quad (3)$$

Taking $d_c^{(0)} = \phi$, and lifting to $n = 4$ dimensions gives

$$d_c^{(4)} = (1/d_c^{(0)})^{4-1} = 4 + \phi^3 = 1/\phi^3 = 4.236067977 = \langle \text{Dim}E - \infty \rangle_H \quad (4)$$

Thus *the expectation value of the Hausdorff dimension of \mathcal{E}^∞ universe is the same as that of a universe with a Menger-Urysohn dimension of 4*. That is why \mathcal{E}^∞ is a hierarchical universe that looks and feels 4 dimensional.

VI. HOW \mathcal{E}^∞ RELATES TO PENROSE TILING, AND THE FI-BONACCI SEQUENCE

\mathcal{E}^∞ universe connects with Penrose tiling and the Fibonacci sequence (see [19]) through \mathcal{E}^∞ [17], [21] and the golden mean. The golden mean is an irrational number and like any irrational number it can be approximated by a fraction; for example $\frac{22}{7}$ is quite close to π . The usual way of obtaining such an approximation, using continued fractions, converges

$$\begin{aligned} D_0 &= D(0, 1) = 0 + \phi = \phi \\ D_1 &= D(1, 0) = 1 + (0)\phi = 1 \\ D_2 &= D(0 + 1, 1 + 0) = 1 + \phi = 1/\phi \\ D_3 &= D(1 + 1, 0 + 1) = 2 + \phi = (1/\phi)^2 \\ D_4 &= D(1 + 2, 1 + 1) = 3 + 2\phi = (1/\phi)^3 \\ D_5 &= D(2 + 3, 1 + 2) = 5 + 3\phi = (1/\phi)^4 \\ D_n(a_n, b_n) &= D((a_{n-1}, a - n - 2 + (b_{n-1} + b_{n-2}))\phi = (1/\phi)^{n-1} \end{aligned} \quad (6)$$

It is notable that for D_4 (dimension 4), the Fibonacci number is $(1/\phi)^3 = 4 + \phi^3$, exactly the Hausdorff dimension of a Menger-Urysohn 4-dimensional space. By induction,

$$D_n = (1/\phi)^{n-1} \quad (7)$$

and we get back the bijection formula from \mathcal{E}^∞ algebra (see Eq (3) above):

$$d_c^{(n)} = (1/\phi)^{n-1}$$

Summing random Cantor sets to infinity in the creation of \mathcal{E}^∞ universe is evocative of spacetime being created by actions over all scales, from submicroscopic to macroscopic and beyond, as envisaged *The Rainbow and the Worm, the Physics of Organisms* by one of us (MWH) [24], following Whitehead [2] and Wolfram Schommers [25].

any Menger-Urysohn dimension n to arrive at the correct Hausdorff dimension $d_c^{(n)}$ as follows:

more slowly for ϕ than for any other number, and in this sense ϕ is the most irrational number there is.

In *Noncommutative Geometry* [23], Alain Connes identified Penrose's fractal tiling as a mathematical quotient space (a space of points 'glued together' by an equivalence relationship), with the dimensional function:

$$D(a, b) = a + b\phi \quad (5)$$

where a, b are integers and $\phi = (\sqrt{5} - 1)/2$. Writing $D_n(a_n, b_n)$ where both a_n and b_n satisfy the Fibonacci recurrence relation $x_{n+2} = x_n + x_{n+1}$ and starting with $D_0 = D(0, 1)$ and $D_1 = D(1, 0)$, the following dimensional hierarchy is obtained:

MeN has conjectured that \mathcal{E}^∞ spacetime can also resolve major paradoxes within quantum theory and produce new results as described elsewhere ([26],[27],[28]).

Here, we move on to the role of cycles in the organization of spacetime and why the golden mean seems to be built into the fabric of life and the universe.

VII. CYCLES EVERYWHERE FOR STABILITY AND AUTONOMY

Nature abounds with cycles and oscillations, from subatomic vibrations to planetary motion, solar cycles and galactic rotations. Some, like Penrose and Gurzadyan hold that the Universe cycles through deaths and rebirths, based on data collected by NASA's WMAP (Wilkinson Microwave Anisotropy Probe) and the BOOMERanG balloon experiment in Antarctica [29]. In a recent review, MWH [31] considers the importance of cycles and the golden mean for natural processes. We

provide a brief account here and in the following two sections.

Cycles are intimately tied to the study of dynamical systems, beginning with celestial mechanics. Newton tried to describe the planetary cycles in terms of his laws of motion more than 300 years ago.

Dynamical systems can be treated mathematically as oscillators. A harmonic oscillator has a certain natural frequency. When perturbed by an external force with the same frequency, resonance occurs and the motion of the oscillator becomes unbounded or unstable. For a typical nonlinear oscillator, this happens whenever the frequency of the perturbing force is a *rational* multiple of the natural frequency of the oscillator.

Andrey Kolmogorov (1903-1987), Vladimir Arnold (1937-2010) and Jürgen Moser (1928-1999) were responsible for the the Kolmogorov Arnold and Moser (KAM) theorem. The KAM theorem is very important for understanding how cyclic activities (or oscillators) interact with one another [30].

They were investigating the behaviour of integrable Hamiltonian systems. The trajectories of Hamiltonian systems in phase space are confined to a doughnut shaped surface, an invariant torus. Different initial conditions will trace different invariant concentric tori in phase space, separated by unstable chaotic regions, where the motion is irregular and unpredictable.

An important consequence of the KAM theorem is that for a large set of initial conditions, the motion remains perpetually quasi-periodic, and hence stable. KAM theory has been extended to non-Hamiltonian systems and to systems with fast and slow frequencies.

The KAM theorem become increasingly difficult to satisfy for complex systems with more degrees of freedom; as the number of dimensions of the system increases, the volume occupied by the tori decreases. Those KAM tori that are not destroyed by perturbation become invariant Cantor sets, or Cantori; and the frequencies of the invariant Cantori approximate the golden mean [32].

The golden mean effectively enables multiple oscillators within a complex system to co-exist without blowing up the system. But it also leaves the oscillators within the system free to interact globally (by resonance), which may have important applications even in the study of the brain (see later). To get a better picture, we look at the circle map.

$$\theta_{n+1} = \theta_n + \Omega(K/2\pi) \sin 2\pi\theta_n \quad (9)$$

where the variable θ_{n+1} is computed mod 1 (meaning counting only partial circles, as full circles get back to the starting point), K is the coupling strength and Ω is the external driving frequency. This map is used to describe oscillatory systems from solid state physics to heart rhythms. The circle map tracks the universal behaviour of dynamical systems associated with transition from cycles to chaos via quasi-periodicity.

The most studied circle map involves a ratio of basic frequencies $w = \phi = (\sqrt{5} - 1)/2$, the golden mean critical point at $K = 1$ and $\Omega = \Omega_c = 0.60666106347011$ ($\approx \phi = 0.618033989 \dots$), reported in many experiments.

Circle maps contain some key features. Arnold tongues are regions in the phase space of circle maps with locally constant rational rotation (winding) numbers between the driver and the natural oscillator frequencies, p/q . They were first investigated for a family of dynamical systems defined by Kolmogorov, who proposed this family as a simplified model for driven mechanical rotors described by equation (9). The circle map of the equation exhibits certain regions in the parameters space when it is locked to the driving frequency (phase- locked, or synchronized). Here, θ is interpreted as the polar angle such that its value lies between 0 and 1; the two parameters are K , the coupling strength between the driver and the rotor, and Ω , the driver frequency. A typical map with Arnold tongues is given in Figure 4.

VIII. CYCLES, QUASI-PERIODICITY, GOLDEN MEAN AND CHAOS

Cycles are often represented by the circle map, a graph that maps the circle onto itself. The simplest form is [33],[34]:

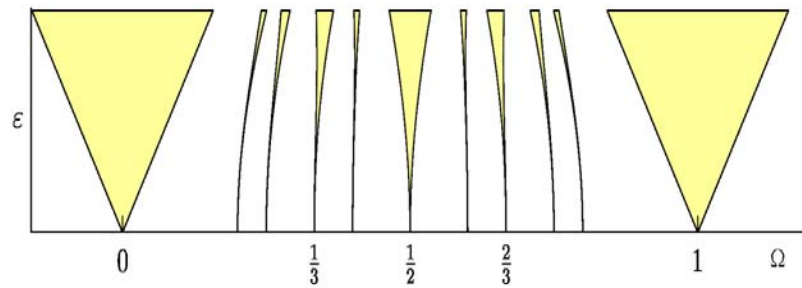


Figure 4 : Some Arnold tongues in the standard circle map $\epsilon = K/2\pi$ versus Ω

For small to intermediate values of K , ($0 < K < 1$), and certain values of Ω , the map exhibits phase locking. In the phase-locked regions, θ_n advances essentially in rational multiples of n ; although it may do so chaotically on the small scale.

The phase-locked regions, called Arnold tongues, are shaded yellow in Figure 4; while the quasi-periodic regions are white. Each yellow V region touches down to a rational value of $\Omega = p/q$ in the limit as $K \rightarrow 0$. The values of (K, Ω) in one of these regions will all result in a motion with rotation number $w = \frac{p}{q}$. For example, all values of (K, Ω) in the middle V region correspond to $w = \frac{1}{2}$. In other words, the sequence stays locked on to the signal despite significant noise or perturbation. This ability to lock on in the presence of noise is central to the utility of phase-locked loop electronic circuits.

The circle map in Figure 4 is invertible or symmetrical around the mid line. For $K > 1$, the circle map is no longer invertible. In Figure 5a [35], the circle map is extended to $K = 4$. Arnold tongues of synchronization are in grey with winding numbers indicated inside the tongue. The white regions are quasiperiodic, and the stippled regions appearing beyond the line $K = 1$ represent *chaos*. This map also depicts fractal self-similarity on different scales. Fractal self-similarity and chaos are closely related. A chaotic system has a fractal dimension and exhibits self-similarity over many scales.

Chaos does not mean random. Mathematically, chaos is sensitive to initial conditions, but it is globally determined in the sense that tends toward a strange attractor (see Appendix 2)

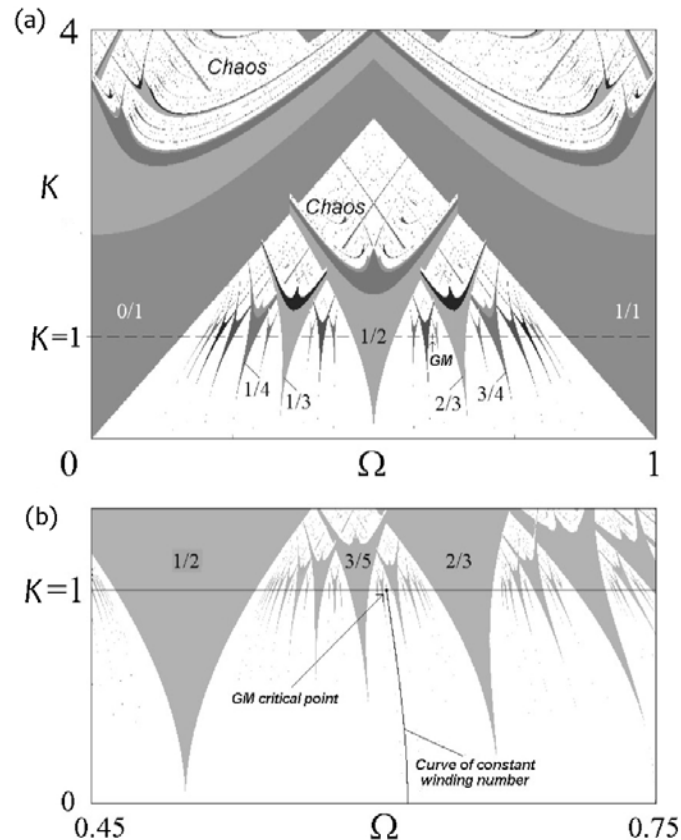


Figure 5 : Extended circle map (see text for details)

The golden mean critical point (GM) is where the curve of constant irrational winding number $\phi = (\sqrt{5} - 1)/2$ terminates on the line $K = 1$ (see Fig 5b), and quasi-periodic behaviour undergoes transition to chaos. This point is marked by an infinite sequence of unstable orbits with periods given by the Fibonacci numbers.

The golden mean is thus located at the edge of chaos, and has a role in keeping the system of oscillators active without interfering with one another as well as away from the state of chaos.

There are claims that the planetary orbits around the sun exhibit golden ratios or ratios according

to the Fibonacci sequence numbers, as many people have commented (see [36] [37] for example). So is our solar system stable? The question is whether it will remain stable as such, at least for billions of years, or transit to chaos much sooner than that. Some astrophysicists claim however, that the planetary orbits are chaotic and sensitive to initial conditions but this means only that they are unpredictable for longer than 100 million years into the future [38] so there is no immediate cause for alarm.

IX. CHAOS AND STRANGE ATTRACTORS

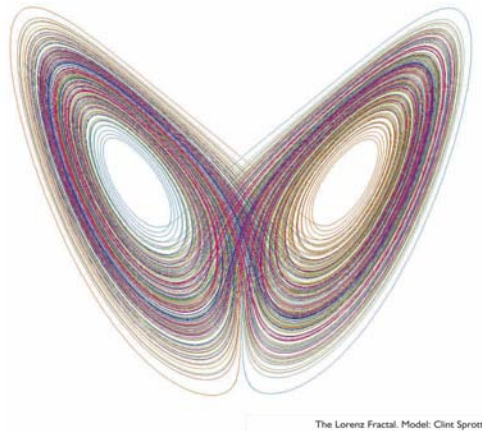


Figure 6 : The Lorenz attractor (from [40])

Edward Lorenz is the generally acknowledged father of chaos theory [39]. According to one account, during the winter of 1961, Lorenz was running a climate model on the computer described by 12 differential equations, when he decided to repeat one of the runs with a small change. Instead of calculating to six decimal digits, he rounded that to three to save computing time, fully expecting to get the same results. But he didn't. That was the beginning of his discovery of the sensitive dependence on initial conditions of chaotic systems, which he described as the butterfly effect. It makes long term weather prediction impossible. His toy equations produced the Lorenz attractor (Figure 6) (the prototype of strange attractors associated with chaotic systems), which bears serendipitous resemblance to butterfly wings, and became the emblem of the chaos era that followed. Numerous strange attractors have been created, mostly as computer artwork, beginning with the book by Clint Sprott [40]. But chaos theory has found applications in meteorology, physics, engineering, economics, biology and medicine.

The Lorenz attractor is a fractal, with self-similar structure on different scales. It has a fractal dimension of 2.06215 and lives in a space of at least 3 dimensions. It contains unstable periodic orbits that can be identified using various mathematical procedures [41], and can also be regarded as twisted or knotted periodic orbits [42].

Chaos theory has been taken up enthusiastically in every field including quantum physics, in the form of quantum chaos, which tries to build a bridge between chaos in classical mechanics and the wavelike motion of electrons in atoms and molecules. Martin Gutzwiller wrote [43]: "The phase space for a chaotic system can be organized at least partially around periodic orbits, even though they are sometimes quite difficult to find."

Chaos is typically found in turbulent flows of fluids, gases, and the atmosphere. Turbulence is traditionally regarded as one of the most intractable problems in physics and mathematics. Mary Selvam first proposed a theory of turbulent fluid flow based on fractal spacetime fluctuations in 1990 (see [44]).

Selvam treats the fractal fluctuations on all spacetime scales as a superposition of a continuum of eddies or vortices. Large scale fluctuations result from the integration of smaller scale fluctuations within, and the growth trajectory traces an overall logarithmic spiral path with the quasi-periodic Penrose tiling pattern for internal structure.

The ratio of radii or circulation speeds corresponding to the successive growth steps of the large eddy generating the geometry of the quasi-periodic Penrose tiling pattern is, of course, equal to the golden mean $\Phi = 1.618 \dots$ ([31]).

Treating turbulence as a continuum of discrete eddies or cycles with Penrose tiling pattern of growth captures key features of biological spacetime, as we shall see.

X. QUANTUM COHERENCE AND CIRCULAR THERMODYNAMICS OF ORGANISMS

In *The Rainbow and the Worm, the Physics of Organisms* [24], MWH presented empirical evidence and theoretical arguments suggesting that organisms are quantum coherent, and derived a circular thermodynamics of organisms that enables organisms to transform and transfer energy with minimum dissipation, which is also implied by quantum coherence. Here, we concentrate on the circular thermodynamic, which depends on a coherent fractal organization of biological spacetime.

The first thing to note is that organisms do not make their living by heat transfer. They are not heat engines, but isothermal systems far away from thermodynamic equilibrium, and depend on the direct transfer of molecular energy by proteins and other macromolecules acting as quantum molecular energy machines at close to 100% efficiency [24].

(It is well-known that enzymes speed up chemical reactions in organisms by a factor of 10^{10} to 10^{23} [45], but they cannot do that without the water that constitutes 70 to 80% of cells and tissues. It is widely recognized that water gives exibility to proteins, reduces the energy barrier between reactants and products and increases the probability of quantum tunnelling by a transient compression of the energy barriers. But there is more to how water actually organizes enzyme reactions in living organisms. Findings within the past decade suggests that interfacial water associated with macromolecules and membranes in cells and tissues is in a quantum coherent liquid crystalline state, and plays a lead role in creating and maintaining the quantum coherence of organisms, as elaborated in *Living Rainbow H₂O* [46] and elsewhere [47],[48].)

For isothermal processes, the change in Gibbs free energy ΔG (thermodynamic potential for doing work at constant temperature and pressure) is,

$$\Delta G = \Delta H - T\Delta S \quad (10)$$

where ΔH is the change in enthalpy (heat content), T is temperature in deg K, and ΔS is the change in entropy.

Thermodynamic efficiency requires that ΔS approaches 0 (least dissipation) and $\Delta H=0$, or $\Delta G=0$ via entropy-enthalpy compensation, *i.e.*, entropy and enthalpy changes cancelling each other out. We shall see how the organism accomplishes that.

XI. A FRACTAL HIERARCHY OF COUPLED CYCLES

For a system to keep far away from thermodynamic equilibrium - death by another name - it must capture energy and material from the environment to develop, grow and recreate itself from moment to moment in a life-cycle, to reproduce and provide for future generations (Figure 7). The key to understanding the thermodynamics of the living system is not so much energy flow as energy capture and storage to create a reproducing life-cycle. The dynamic closure implied by the life-cycle is the beginning of a circular thermodynamics that transforms and transfers energy and materials with maximum efficiency (least dissipation) (see [24], [49]).

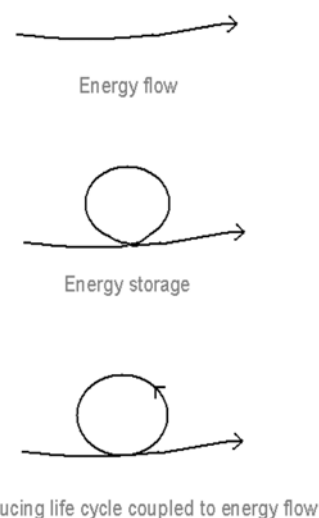


Figure 7 : Life depends on energy capture and storage to form a self-reproducing life-cycle coupled to energy flow

The life-cycle is a fractal hierarchy of self-similar cycles organised by the characteristic spacetimes of the processes involved. All real processes have characteristic spacetimes. In the organism, the heart (10^{-1} m) beats in a second, nerve cells (10^{-4} m) fire in a tenth of a second or faster, and protons (10^{-15} m) and electrons (10^{-17} m) move in 10^{-12} to 10^{-15} s. Cells divide in minutes, and physiological processes have longer cycles of hours, a day, a month or a year.

The coherent fractal hierarchy of living activities arises because processes with matching space times interact most strongly through resonance, and also link up to the entire hierarchy. That is why biological activities come predominantly in cycles or biological rhythms. (In the language of quantum physics, the organism is a superposition of coherent quantum activities over all spacetimes [24].) The possibility for cycles in the living world coupling and linking up to cycles in the physical universe is surely why life is

possible, and indeed some would argue, as Whitehead did [2], that the entire universe is alive.

The coupled cycles form a nested fractal self-similar structure. The lifecycle consists of smaller cycles each with still smaller cycles within, spanning characteristic spacetimes from sub-nanometre to metres and from 10^{-15} s to hours and years (Figure 8).

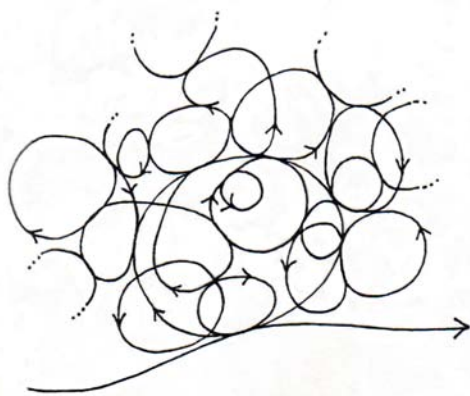


Figure 8 : The fractal structure of coupled activity cycles in living systems

XII. MINIMUM ENTROPY PRODUCTION

Cycles enable the activities to be coupled together, so that energy yielding processes can transfer energy directly to those requiring energy; and the direction can be reversed when necessary. This cooperativity and reciprocity resulting from the fractal hierarchy of coupled cycles is an extended form of Onsager reciprocity relation that conventionally applies strictly only to near-equilibrium steady state (see [24] for details). What it means in practice is that energy can be concentrated to any local point where it is needed, and conversely spread globally from any local point. In that way, the fractal hierarchy of coupled cycles maximizes both local autonomy and global cohesion, which is the hallmark of quantum coherence [24] according to the criterion of factorisability defined by Glauber [50].

To get an idea of such coupled cycles, one needs to look no further than charts of biochemical metabolic pathways [51]. Most if not all of the reactions go either way, depending on the local concentrations of reactants and products. In further accord with circular thermodynamics, biochemical recycling is ubiquitous; there are numerous scavenging or salvaging pathways for the recovery of building blocks of proteins, nucleic acids, glycolipids, and even entire proteins.

The fractal hierarchy of coupled cycles confers dynamic stability as well as autonomy to the system on every scale. Thermodynamically, no net entropy is generated in the case of perfect cycles; and the system maintains its organization.

The fractal structure effectively partitions the organism into a hierarchy of systems within systems *defined by the extent of equilibration of (dissipated) energies*. Thus, energies equilibrated or evenly spread within a smaller spacetime will still be out of equilibrium in the larger system encompassing the first, and hence capable of doing work.

There are now two ways to mobilize energy efficiently with entropy change approaching zero: very slowly with respect to the characteristic time so it is reversible at every point, or very rapidly with respect to the characteristic time, so that in both cases the energy remains stored (in a coherent non-degraded form) as it is mobilized. Consequently, the organism *simultaneously* achieves the most efficient equilibrium and far-from-equilibrium energy transfer.

The nested dynamical structure also optimises the kinetics of energy mobilisation. For example, biochemical reactions depend strictly on local concentrations of reactants, which are extremely high, as their extent of equilibration is typically at nanometre dimensions (in nanospaces).

In the ideal - approached most closely by the healthy mature organism and the healthy mature ecosystem - an overall internal conservation of energy and compensation of entropy ($\Sigma \Delta S = 0$) is achieved. In this state of balance, the system organization is maintained and dissipation minimized; i.e., the entropy exported to the environment also approaches zero, $\Sigma \Delta S \geq 0$ (Figure 9).

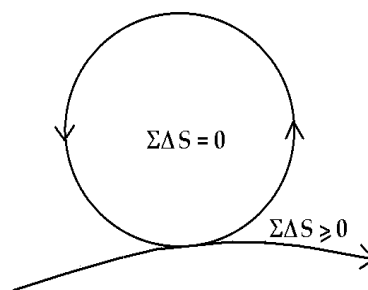


Figure 9 : The zero-entropy ideal of circular thermodynamics

Internal entropy compensation (and energy conservation) implies that there needs to be free variation in microscopic states within the macroscopic system; *i.e., the internal microscopic detailed balance at every point of classical steady state theory is violated.* (This is also the basis of the extension of Onsagers reciprocity relationship to far from equilibrium condition.)

For an organism, this means that detailed energy balance is not necessary at every point. Most often, parts of it are in deficit, and severely so, when one needs to run from a tiger knowing the energy can be replenished after a successful escape. The same applies to ecosystems: all species are in a sense storing

energy and resources (nutrients) for every other species via complex food webs and other symbiotic relationships.

The above considerations give rise to the prediction that a sustainable system maximizes cyclic, non-dissipative flows while minimizing dissipative flows, *i.e.*, it tends towards *minimum entropy production* even under far from equilibrium conditions, as conjectured by Ilya Prigogine [52].

Such a system has a hierarchy of coherent energy storage spacetimes so that within the coherence volume, there is no time separation, and within the coherence time, there is no space separation. Thus, organic spacetime exists as a hierarchy of simultaneities, or durations, precisely as envisaged by Bergson [5] and Whitehead [2],[6]. (See [24] for a more detailed discussion).

The golden mean most likely enters into the fractal structure in the form of the golden fractal. As the most irrational of all numbers (see Section 6 above), it allows the maximum number of non-resonating activities to co-exist (representing maximum coherent energy storage). On the other hand, it is also arbitrarily close to a maximum number of rational numbers so specific resonances can easily be established for energy transfer.

We shall see more clearly how the golden fractal of neuronal activities are the key to optimum intercommunication and information processing in the final section. The next section shows how fractals are mathematically isomorphic to quantum coherent states.

XIII. FRACTALS AND QUANTUM COHERENCE

The coherent fractal structure maximizes global connectivity and local autonomy, the hallmark of quantum coherence, as mentioned earlier. One of the authors (GV) has shown that a functional representation of self-similarity – the most important property of fractal structures – is mathematically isomorphic with squeezed quantum coherent states [53, 54, 55], in which Heisenberg's uncertainty is minimum. Quantum coherence thus seems to underly the ubiquitous recurrence of fractal self-similarity in Nature.

Let us see how this works with the logarithmic spiral, and the special case of the golden spiral, as an example. The golden spiral and its relation to the Fibonacci sequence are of great interest because the Fibonacci sequence appears in many phenomena, ranging from botany to physiological and functional properties in living systems, as the “natural” expression in which they manifest themselves.

The defining equation for the logarithmic spiral in polar coordinates (r, θ) is [56, 57]:

$$r = r_0 e^{d\theta} \quad (11)$$

with r_0 and d arbitrary real constants and $r_0 > 0$. In a log-log plot with abscissa $\theta = \ln e^\theta$ the spiral is represented by a straight line with slope d

$$\ln \frac{r}{r_0} = d\theta. \quad (12)$$

The (fractal) self-similarity property of the logarithmic spiral is manifest in the constancy of the angular coefficient $\tan^{-1}d$: rescaling $\theta \rightarrow n\theta$ affects r/r_0 by the power $(r/r_0)^n$.

The logarithmic spiral is called the *golden spiral* when at $\theta = \pi/2$ we have $r/r_0 = e^{d(\pi/2)} = \Phi$, where Φ denotes the golden mean $(1 + \sqrt{5})/2$. We may introduce the subscript g (denoting *golden*) and put $d_g \equiv (\log \Phi)/(\pi/2)$. The polar equation for the golden spiral is thus $r_g(\theta) = r_0 e^{d_g \theta}$. The radius of the golden spiral increases in geometrical progression with the ratio Φ as θ increases by $\pi/2$: $r_g(\theta + n\pi/2) = r_0 e^{d_g(\theta + n\pi/2)} = r_0 e^{d_g \theta} \Phi^n$ and $r_{g,n} \equiv r_g(\theta = n\pi/2) = r_0 \Phi^n$, $n = 0, 1, 2, 3, \dots$

The so called Fibonacci tiling provides a tool for a good approximate construction of the golden spiral. The Fibonacci tiling is obtained by drawing in an appropriate way [56] squares whose sides are in the Fibonacci progression, 1, 1, 2, 3, 5, 8, 13, ... (the sequence is defined by the relation $F_n = F_{n-1} + F_{n-2}$, with $F_0 = 0$; $F_1 = 1$). The Fibonacci spiral is then made from quarter-circles tangent to the interior of each square. It does not coincide exactly with the golden spiral because $F_n/F_{n-1} \rightarrow \Phi$ in the $n \rightarrow \infty$ limit, but is not equal to Φ for n finite.

The golden ratio Φ and its “conjugate” $\psi \equiv 1 - \Phi = -1/\Phi = (1 - \sqrt{5})/2 = -\phi$ are both solutions of the quadratic equation

$$x^2 - x - 1 = 0 \quad (13)$$

and of the recurrence equation $x^n - x^{n-1} - x^{n-2} = 0$, which, for $n = 2$, is the relation (13). This is satisfied also by the geometric progression with ratio Φ of the radii $r_{g,n} = r_0 \Phi^n$ of the golden spiral. Eq. (13) is the characteristic equation of the differential equation $r + \dot{r} - r = 0$, which admits as solution $r(t) = r_0 e^{i\omega t} e^{+d\theta(t)}$ with $\omega = \pm i\sqrt{5}/2$ and $\theta = -t/(2d) + c$ with c , r_0 and d constants. By setting $c = 0$, $r(t) = r_0 e^{\mp\sqrt{5}t/2} e^{-t/2}$, *i.e.* $r_\Phi(t) = r_0 e^{-\Phi t}$ and $r_\psi(t) = r_0 e^{-\psi t}$.

Consider now the parametric equations of the logarithmic spiral Eq. (11):

$$x = r(\theta) \cos \theta = r_0 e^{d\theta} \cos \theta \quad (14a)$$

$$y = r(\theta) \sin \theta = r_0 e^{d\theta} \sin \theta \quad (14b)$$

The point $z = x + iy = r_0 e^{d\theta} e^{i\theta}$ on the spiral is completely specified in the complex z -plane only when the sign of $d\theta$ is assigned. The completeness of the (hyperbolic) basis $\{e^{-d\theta}, e^{+d\theta}\}$ requires that both

the factors $q = e^{\pm d\theta}$ must be considered. In many instances the so-called direct ($q > 1$) and indirect ($q < 1$) spirals are both realized in the same system (e.g. in phyllotaxis studies).

We thus consider the points $z_1 = r_0 e^{-d\theta} e^{-i\theta}$ and $z_2 = r_0 e^{+d\theta} e^{+i\theta}$. For convenience (see below) opposite signs for the imaginary exponent $i\theta$ have been chosen. Using the parametrization $\theta = \theta(t)$, z_1 and z_2 are found to be solutions of the equations

$$m \ddot{z}_1 + \gamma \dot{z}_1 + \kappa z_1 = 0, \quad (15a)$$

$$m \ddot{z}_2 - \gamma \dot{z}_2 + \kappa z_2 = 0 \quad (15b)$$

respectively, provided the relation

$$\theta(t) = \frac{\gamma}{2md} t \equiv \frac{\Gamma}{d} t \quad (16)$$

holds (where we have neglected an arbitrary additive constant). We see that $\theta(T) = 2\pi$ at $T = 2\pi d/\Gamma$. In Eqs. (15) a dot denotes derivation with respect to t ; m, γ and κ are positive real constants. The notations $\Gamma \equiv \gamma/2m$ and $\Omega^2 = (1/m)(\kappa - \gamma^2/4m) = \Gamma^2/d^2$, with $\kappa > \gamma^2/4m$, have been used. The parametric expressions $z_1(t)$ and $z_2(t)$ for the logarithmic spiral are thus $z_1(t) = r_0 e^{-i\Omega t} e^{-\Gamma t}$ and $z_2(t) = r_0 e^{+i\Omega t} e^{+\Gamma t}$, solutions of Eqs. (15a) and (15b). At $t = nT$, $z_1 = r_0 (e^{-2\pi d})^n$, $z_2 = r_0 (e^{2\pi d})^n$, with the integer $n = 1, 2, 3, \dots$

This suggests that t can be interpreted as the time parameter and the time-evolution of the direct and indirect spirals is described by the equations (15a) and (15b). The “two copies” (z_1, z_2) can be viewed as the evolution forward in time and backward in time, respectively. The “angular velocity” of (the growth of) the spiral is given by $|d\theta/dt| = |\Gamma/d|$.

By putting $[z_1(t) + z_2^*(-t)]/2 = x(t)$ and $[z_1^*(-t) + z_2(t)]/2 = y(t)$, we reduce eqs. (15a) and (15b) to the pair of damped and amplified harmonic oscillators:

$$m\ddot{x} + \gamma\dot{x} + \kappa x = 0, \quad (17a)$$

$$m\ddot{y} - \gamma\dot{y} + \kappa y = 0 \quad (17b)$$

respectively. The second of these is the *time-reversed* image ($\gamma \rightarrow -\gamma$) of the first and the global system ($x - y$) is a *closed* system. We see that the oscillator x is a dissipative, *open* (non-hamiltonian) system and in order to set up the canonical formalism we need to *double* the degrees of freedom by introducing its time reversed image y [58]: the physical meaning of the requirement to consider both the elements of the basis $\{e^{-d\theta}, e^{+d\theta}\}$ is that we need to consider the *closed* system (z_1, z_2). Only then can we set up the canonical formalism.

If we did not close the system z_1 with the system z_2 , we would not be able to define the conjugate momenta because the Lagrangian would not exist.

We now remark that classical, deterministic systems presenting loss of information (dissipation) might, providing some constraints are imposed, behave according to quantum evolution [59, 60, 61]. In the present case, this means that the logarithmic spiral and its time-reversed double (the direct and the indirect spiral) manifest themselves as *macroscopic quantum systems*. The quantization of the system described by Eqs. (15a) and (15b) (or (17a) and (17b)), can be performed in the usual way and the result is that the system ground state $|0(t)\rangle$ is a coherent squeezed state, which is produced by condensation of couples of (entangled) A and B modes (related to the (z_1, z_2) couple, see Ref. [58, 54, 55]) for details): $(AB)^n$, $n = 0, 1, 2, \dots, \infty$. The operator which generates $|0(t)\rangle$ is recognized to be the two mode squeezing generator with squeezing parameter $\zeta = -\Gamma t$. It must be stressed that the correct mathematical framework to study quantum dissipation is the one of quantum field theory (QFT). The realization of the logarithmic spiral (and in general of fractals) in the many cases observed in nature involves indeed an infinite number of elementary degrees of freedom.

We may define the *fractal Hamiltonian*, which turns out to be actually the *fractal free energy* for the coherent boson condensation process out of which the fractal is formed. We indeed find that time evolution is controlled by the *entropy* operator. This is to be expected because entropy controls time irreversibility and the breakdown of time-reversal symmetry that is characteristic of dissipation is clearly manifest in the formation process of fractals. In the case of the logarithmic spiral, the breakdown of time-reversal symmetry is associated with the chirality of the spiral: the indirect (right-handed) spiral is the time-reversed, *but distinct*, image of the direct (left-handed) spiral.

These results can be also extended to other examples of deterministic fractals [54], such as the Koch curve, the Sierpinski gasket and carpet, the Cantor set, etc.. We do not consider these cases here. We only recall that by resorting to the results reported above the isomorphism can be shown [55] to exist between classical and quantum electrodynamics, from one side, and the fractal self-similarity structure and squeezed coherent states, from the other side, provided some quite general conditions are satisfied.

As suggested also in the discussion above (see also [24] and below), the paradigm of coherence seems to extend to large part, if not the whole of the universe [62, 54, 55].

XIV. TOPOLOGY OF QUANTUM SPACETIME

The isomorphism between quantum coherence and fractals goes considerably deeper than we have presented so far. In a series of earlier papers (see [63]-[66]), MeN showed that \mathcal{E}^∞ theory gives predictions of

the mass spectrum of elementary particles and quarks in high energy physics based on the golden mean that are in remarkable agreement with those generally accepted experimentally and theoretically in the literature. Further, the same predictions are provided by a physical interpretation of four-dimensional fusion algebra, of Conne's non-commutative geometry and related theories such as Freedmann topological theory of four manifolds (wild topology), and Penrose space X (of which \mathcal{E}^∞ is a higher dimensional space). The fascinating details are beyond the scope of the present paper. We cite the results because they so strongly suggest that the mass spectrum based on the golden mean is a reflection of the quantum topology of spacetime [65].

This conjecture is reinforced, as MeN pointed out, in the simplest mechanical model for \mathcal{E}^∞ theory, which is two golden mean coupled-oscillators, with frequencies of vibrations $\omega_1 = \phi$, $\omega_2 = 1/\phi$. That is because at least in the case of quarks, what we consider to be a particle can be thought of as a highly localized vibration, a standing wave simulating a particle (as in string theory).

Generalizing to n such nested oscillators, Leila Marek-Crnjac was able to use Southwell and Dunkerley summation theorems for structural stability to obtain the masses of the elementary particles of the standard model, as well as the current quarks and constituent quarks [67]. The results are again very close to the theoretical and experimental masses found previously.

Marek-Crnjac also noted that the golden mean plays a central role in dynamic stability in KAM theory (see above), pointing out that string theory eliminates the wave-particle duality by using the highly localized vibration of a Planck length string that gives rise to a particle when perceived on lower energy levels [67]. In this way, the golden mean enters into the mass spectrum via the KAM theory. As it is the most irrational number (see sections 6 and 12) it plays the key role in the stability of periodic orbits and the onset of global chaos. The ratio of Ω/ω (driver to oscillator frequency) is decisive as to whether the motion is localized (regular) or dissipative (stochastic). If the ratio is rational, the torus is destroyed. However, if it is irrational, the torus persists. A well-known application of this theory is the Kirkwood gaps - dips in the distribution of the main belt asteroids, which coincide with orbital resonances with Jupiter. What this means is that a particle is observed only when the energy is localized in a highly coherent vibration in an irrational frequency, and the most irrational frequency is ϕ .

Marek-Crnjac's argument applies also to the circular thermodynamics of organisms and the fractal hierarchy of living activities developed in Sections 7-12. The mass spectrum of elementary particle and living activities are both a reflection of the universal quantum topology of spacetime.

XV. COHERENT BRAIN WAVES, SCALE-FREE LAWS AND FRACTALS

Laboratory observations on the brain have consistently detected spatially extended regions of coherent neuronal activities, most thoroughly described in recent years by Walter Freeman and colleagues [68],[69],[70]. These phenomena have been observed by Lashley since the 1940s, who introduced the notion of field. Karl Pribram proposed his holographic hypothesis of memory formation in the early 1960s that introduced the notion of coherence in analogy to laser theory [58]. Hiroomi Umezawa proposed the first quantum field theory of memory in 1967 (see [71],[72]), that includes both the notions of field and coherence.

Observations clearly show that the coherent cortical activities cannot be fully accounted for by the electric field of the extracellular dendritic current or the extracellular magnetic field from the high-density electric current inside the dendritic shafts, nor by chemical diffusion. Spatially extended patterns of phase-locked oscillations are intermittently present in resting, awake subjects, and in the same subjects actively engaged in cognitive tasks. They are best described as properties of the brain modulated upon engagement with the environment. These packets of waves extend over spatial domains covering much of the hemisphere in rabbits and cats [73]-[76] and over regions of 19 cm linear dimension in the human cortex with near zero phase dispersion [68], [77]-[79].

Umezawa's many-body model [80] is based on the quantum field theoretic notion of spontaneous breakdown of symmetry [81],[61], which requires the existence of Nambu-Goldstone (NG) massless particles. Examples are the phonon modes in crystals, the magnon modes in ferromagnets, etc. They can be described, as customary in quantum theory, as the quanta associated with certain waves such as the elastic wave in crystals, the spin wave in ferromagnets. The role of such waves is that of establishing long range correlation. The mechanism of spontaneous breakdown of symmetry generates the change of scale: from the microscopic scale of the elementary constituent dynamics to the macroscopic scale of the system observable ordered patterns. In ferromagnets, for example, the ordered patterns is described by magnetization, which for this reason is called the order parameter. The phase transition from zero magnetization to the magnetic phase is induced by some external weak magnetic field. The mathematical structure of the theory must be adequate to allow for physically distinct phases. Quantum field theory possesses such a mathematical structure. The ground states corresponding to physically distinct phases are characterized by distinct degrees of ordering described by different densities of NG modes condensed in them. Such a condensation of NG modes

in the ground states is a coherent condensation, which physically expresses the in phase synchronized oscillations. In quantum mechanics, on the contrary, all the state representations are physically equivalent and therefore not useful to describe phase transitions [82].

The quantum variables relevant to the many-body model of the brain have been identified to be the electric dipole vibration modes of the water molecules that constitute the matrix in which neurons and glia cells are embedded [83],[84]. The spontaneous breakdown of the rotational symmetry of electrical dipoles of water and other molecules implies the existence of NG modes. These modes have been called the dipole wave quanta (DWQ). The system ground state is thus obtained in terms of coherent condensation of the DWQ, which are the agents responsible for neuronal coordination [83]-[85]. In particular, it is found that the memory state is a squeezed coherent state for the basic quantum variables expressed mesoscopically as amplitude and phase modulation of the carrier signal observed in electroencephalograms (EEGs) and electrocorticograms (ECoGs).

Laboratory observations show that self-similarity characterizes the brain ground state. Measurements of the durations, recurrence intervals and diameters of neocortical EEG phase patterns have power-law distribution with no detectable minima. The power spectral densities in both time and space conform to power law distribution [73],[74], a hallmark of fractals. It is therefore consistent with the squeezed coherent state for memory found earlier.

Coherent signals are obtained when the electrodes are closely spaced. A lot of data have been collected by Freeman's group on ECoG spatial imaging coming from small, high-density electrode arrays fixed on the surfaces of the olfactory, visual, auditory, or somatic modules. Spectral analysis of the ECoG shows broad distribution of the frequency components, where the temporal power spectral density in log-log coordinates is power-law, $1/f^\alpha$, in segments. Below an inflection in the theta-alpha range the power spectral density is at, $\alpha = 0$. Above, the \log_{10} power decreases linearly with increasing \log_{10} frequency in the beta-gamma range (12.5 - 80 Hz) with the exponent α between 2 and 3. One can show that in slow-wave sleep, the exponent averages near 3; in seizures it averages near 4. On the basis of what was said above, such values of the slope α provide corresponding values of the fractal dimension $d \equiv \alpha$, with deformation parameter $q \equiv 1/f^\alpha$ and coherent strength corresponding to the power spectral density. Brief epochs of narrow band oscillation create multiple peaks, indicating a departure from the scale free regime (the straight line) and therefore the presence of structures emergent from the background activity.

The observed power law signals the scale free ("spatial similarity") property of the brain ground states.

The spatial similarities reveal the long spatial distances across which synaptic interactions can sustain coherence, namely the high-density coordination of neuron firing by synaptic interaction, in agreement with the dissipative model prediction.

A confirmation of the brain scale-free behaviour comes also from the group of Dietmar Plenz at the US National Institute of Mental Health. They have identified neuronal avalanches - cascades of neuronal activities that follow precise $1/f$ power laws - in the excitatory neurons of the superficial layers in isolated neocortex preparations *in vitro* as well as in awake animals and humans *in vivo* [86]. They showed that the neuronal avalanche of the default state with the $1/f$ signature of self-organized criticality gives the optimum response to inputs as well as maximum information capacity (reviewed elsewhere in more detail by MWH [87]).

Most significantly, the avalanche dynamics give rise to coherence potentials consisting of subsets of avalanches in which the precise waveform of the local field potential is replicated with high fidelity in distant network sites. The process is independent of spatial distance and includes near instantaneous neuronal activities as well as sequential activities over many time scales.

Most coherence potentials are spatially disjunct. Local Field Potentials (LFPs) of successive coherence potentials are not similar, but they are practically identical within a coherence potential among all the participating sites, there being no growth or dissipation during propagation. This suggests that the waveform of a coherence potential is a high-dimensional coding space in information processing of the brain. For decades, phase-locked neuronal activity has been reliably recorded using the LFPs or EEG and was found to correlate with the presentation of stimulus in animals and visual perception in humans.

XVI. GOLDEN MUSIC OF THE BRAIN

In living systems, fractals must satisfy the state of quantum coherence which maximizes global cohesion as well as local autonomy, and enables energy from any local level to spread to the global and conversely concentrate energy to any domain from the entire system. Our discussion suggests that fractals with fractal dimension in the golden mean (golden fractals) might be the most effective in giving autonomy to the greatest number of cycles. On the other hand, global cohesion is also ensured, because cycles in a fractal hierarchy are quantum coherent; energy can be shared between global and local. The golden mean is also close to an infinite number of rational ratios, so special resonances or correlations can be easily established. Thus, one would expect biological rhythms in general to conform to the golden mean, although no such survey has yet been carried out. The golden mean figures

prominently in the EEG frequencies of the resting brain (see Table 1). Belinda Pletzer, Hubert Kerschbaum and Wolfgang Klimesch proposed that brain frequencies that never synchronize in the resting brain may play an important role in the organization of groups of cells in

keeping their rhythms distinct and free from mutual interference. They suggested that this can be achieved via frequencies in irrational multiples in the resting (default) brain [88] (see also [87]). Table 1 lists the typical EEG frequency bands.

Table 1 : Typical EEG frequency bands and subbands and corresponding periods (from [88]).

Band	(Hz)	Subband	(Hz)	Peak (Hz)	Period (ms)
delta	1.5-4	delta 1	1-2	1.5	667
		delta2	2-3	2.5	400
theta	4-10	theta1	3-5	4	250
		theta2	5-8	6.5	154
alpha	8-12	alpha	8-12	10	100
beta	10-30	beta1	12-20	16	62.5
		beta2	20-30	25	40
gamma	30-80	gamma1	30-50	40	25
		gamma2	50-80	65	15
fast	80-200	ripples1	80-120	100	10
ripples		ripples2	120-200	160	6.25

The classical EEG frequency bands can indeed be described as a geometric series with a ratio between neighbouring frequencies approximating $\Phi = 1.618$, and the successive frequencies are the sum of two previous ones, as in the Fibonacci sequence. Intuitively at least, one can see that the golden mean provides the highest physiologically possible desynchronized frequencies, and at the same time, the potential for spontaneous diverse coupling and uncoupling between rhythms and a rapid transition from resting state to activity.

A team of researchers led by Miles Whittington have been studying the intricacies in the golden music of the brain by recording from multiple layers of the neocortex simultaneously. They found multiple local neuron assemblies supporting different discrete frequencies in the neocortex network, and the relationships between different frequencies appear designed to minimize interference and to allow diverse coupling of activities via stable phase interactions and the control of the amplitude of one frequency in relation to the phase of another [89].

The $1/f$ pattern of EEG is really a time-averaged smoothed collection of multiple, discrete frequencies, and does not represent all the frequencies and combination of frequencies present in the brain. (It is like a recording of a Mozart symphony that averages out all the sounds made in discrete periods of time, so the music is completely buried.) Detailed observations made by the team have shown that at least three discrete frequencies δ (1-3 Hz), θ (6-9 Hz), and γ (30-50 Hz) are often expressed simultaneously, and can be associated with further much slower rhythms both *in vivo* and *in vitro*.

Discrete frequencies ranging from low δ to high γ can be produced from a single area of the isolated neocortex *in vitro*, with peak frequencies distributed according to the golden mean.

To keep simultaneously occurring frequencies apart and minimize interferences, the solution is indeed to have ratios of frequencies that are irrational numbers. Coexistent γ_1 and β_2 rhythms in the cortex, for example, are generated in two different layers and survive physical separation of the layers. The ratio of peak frequencies is approximately Φ , resulting in a periodic pattern of change in low-level synchrony between the layers with a period equal to the sum of the two periods of oscillation present. This phenomenon can occur to some extent with any pair of co-expressed frequencies. But using Φ as a common ratio between adjacent frequencies in the EEG spectrum enables the neocortex to pack the available frequency space (thereby maximising the information processing capacity, or the capacity to produce the most music). If the cortex uses different frequency bands to process different aspects of incoming information, then it must also have the ability to combine information held in these bands to reconstruct the input; hence the importance of keeping them separate, as the golden mean does.

It is also possible for a local neuron assembly generating a single frequency rhythm to switch frequencies. Such changes are facilitated by a range of mechanisms including changes in neuronal intrinsic conductances and non-reciprocal interactions with other regions oscillating at a similar frequency. After stimulation, γ frequencies can transform to β frequencies

(approximately halved) due to inhibitory postsynaptic potentials on the principal cells generating the action potentials.

Can interactions between multiple spatiotemporal scales of activity tell us anything about how the cortex processes sensory information?

In the time domain, the ability to distinguish rapidly changing features of an input from more slowly changing features provides an efficient means of recognizing objects. Feature detection over a range of time scales can reproduce many properties of individual neurons in the visual cortex. Thus, from a computational perspective, it is an advantage for the cortex to process different temporal scales of information separately, using different frequencies. It has been shown that rhythms with larger temporal scales (slower frequencies) facilitate interactions over greater distances in cortical networks, i.e., they may synchronize over larger areas of the visual map in the retina of the eyes. Thus, different frequencies may have a role for processing sensory information on different spatial scales. In a visual task designed to test perception shifting from features of an object with low spatial frequency to those with high spatial frequency, a direct correlation was found between the spatial scale of the sensory object and the temporal scale (frequency) of associated cortical rhythms. Thus cross-frequency phase synchronization is a possible means of combining information from different frequency channels to fully represent a sensory object.

VII. CONCLUSION

We have considered the fabric of spacetime from the widest perspectives, drawing on findings from mathematics, quantum physics, far from equilibrium thermodynamics, biology, and neurobiology. Although a definite answer cannot be given to the question asked in the title of this paper, the totality of findings obtained by different authors discussed in previous Sections seem to converge and justify our speculation that spacetime is fractal and quantum coherent in the golden mean. Mathematically, the fractal universe is non-differentiable and discontinuous, yet dense in infinite dimensional spacetime. Physically, it is a quantum coherent universe consisting of an infinite diversity of autonomous agents all participating in co-creating organic, fractal space-time by their multitudinous coupled activity cycles. Biologically, this fractal coherent space-time could also provide the fabric of conscious awareness mirrored in the quantum coherence of our brain states. This view depicts a new organic cosmogony consonant with that of Alfred North Whitehead [1], resolving major paradoxes associated with the classical mechanics, and paving the way to reconciling or transcending quantum theory and general relativity. Much work remains to be done in order to provide a definitive answer to our

question of whether fractal self-similarity, golden ratio and coherence are characterizing features of the fabric of spacetime.

As this manuscript is going to press, the first ever observation is reported that the brightness of some stars pulsate at primary and secondary frequencies whose ratios are near the golden mean [John F. Lindner, Vivek Kohar, Behnam Kia, Michael Hippke, John G. Learned, and William L. Ditto, Strange Nonchaotic Stars, *Phys. Rev. Lett.* 114, 054101 (2015). arxiv.org/abs/1501.01747]. This evidence of strange nonchaotic dynamics recorded by the Kepler space telescope lends support to our vision of the fractal golden mean structure of spacetime.

VIII. ACKNOWLEDGMENT

We thank Peter Saunders for stimulating and helpful discussions and for critical reading of successive drafts of this manuscript.

APPENDIX 1. ZENO'S PARADOX

Achilles is running a race with the tortoise. Achilles gives the tortoise a head start of 100 metres, say. If we suppose that both run at constant speed – Achilles very fast and the tortoise very slow – then after some time, Achilles will have run 100 metres, bringing him to the tortoise's starting point. But during that time, the tortoise has run a much shorter distance, say 10 metres. It will then take Achilles some further time to run that distance, by which time the tortoise will have gone ahead farther; and then he would need more time still to reach that third point, while the tortoise moves ahead, and so on. Thus, whenever Achilles reaches somewhere the tortoise has been, he still has farther to go. Therefore, because there are an infinite number of points where the tortoise has already been for Achilles to reach, he can never overtake the tortoise [4].

APPENDIX 2. SOME INFORMAL DEFINITIONS

We provide here informal definitions (from [8]) of some mathematical terms that will be used in this paper; some, like deterministic chaos, have no generally agreed definition.

Set theory is the branch of mathematical logic about collections of mathematical objects. The modern study of set theory was initiated by German mathematicians Georg Cantor (1845-1918) and Richard Dedekind (1831-1916) in the 1870s. A *closed set* contains its own boundary, its complement is an *open set* which is a set that does not contain its boundary.

A *Borel set* is any set in a topological space that can be formed from open sets (or equivalently from closed sets) through the operations of countable union, countable intersection, and relative complement.

A *countable set* is a set with the same number of elements as some subset of the set of natural numbers. The elements of a countable set can be counted one at a time, and although the counting may never finish, every element of the set will eventually be associated with a natural number.

The *union* of two sets A and B is the set of all elements that belong to either set and is denoted by $A \cup B$. The *intersection* of A and B is the set of all elements that belong to both sets and is denoted by $A \cap B$. The *relative complement* of A in B is the set of elements that are in B but are not in A .

A *bijection* is a mapping from a set A to a set B that is both an *injection* (one-to-one) and a *surjection* (onto); it relates each member of A (the domain) to a unique member of B (the range). Each element of B also has a unique corresponding element in A .

The classical triadic *Cantor set* is obtained by dividing the unit line into three equal parts, discarding the middle part except for its end points, and repeating the operation with the two remaining parts *ad infinitum*. In the random version, it could be any of the three parts that is discarded at random after each division. A *topological space* is a set of points and a set of neighbourhoods for each point that satisfy a set of axioms relating to points and neighbourhoods. The definition of a topological space relies only on set theory and is the most general notion of a mathematical space.

For our purposes, the *topological dimension* is what one ordinarily understands by the concept of dimension. A point has topological dimension 0, a curve has topological dimension 1 (whether it is closed up into a circle or not); a sheet has a topological dimension of 2, as do the surface of a cylinder, sphere or doughnut, and so on.

The *Menger-Urysohn* dimension is a generalized topological dimension of topological spaces, arrived at by mathematical induction. It is based on the observation that, in n -dimensional Euclidean space R^n , the boundaries of n -dimensional balls have dimension $n-1$. Therefore it should be possible to define the dimension of a space inductively in terms of the dimensions of the boundaries of suitable open sets.

The *Hausdorff dimension* generalizes the notion of dimension to irregular sets such as fractals. For example, a Cantor set has a Hausdorff dimension of $\log 2 / \log 3$, the ratio of the logarithm to the base 2 of the parts remaining to the whole after each iteration.

A *fractal* is a mathematical set that typically displays self-similar patterns, and has dimensions that are fractions rather than integers. Geometric examples are branching trees, blood vessels, frond leaves etc.

Deterministic Chaos describes dynamical systems with unpredictable behavior that is highly sensitive to initial conditions, but nevertheless globally determined in the sense that the trajectories are

confined within a region of phase space called *strange attractors*.

REFERENCES RÉFÉRENCES REFERENCIAS

1. Ho MW. Golden geometry of E-infinity fractal spacetime. Story of phipart 5. *Science in Society* 2014, **62**, 36-39.
2. Whitehead AN. *Science and the Modern World, Lowell Lectures 1925*, Collins Fontana Books, Glasgow, 1975.
3. Penrose R. *The Road to Reality, A Complete Guide to the Laws of the Universe*, Vintage Books, London, 2005. 1099 pp.
4. Wikipedia. Zeno's paradoxes. 20 October 2014.
5. Bergson H. *Time and Free Will, An Essay on the Immediate Data of Consciousness* (FL Pogson trans.), George Allen & Unwin, Ltd., New York, 1916.
6. Whitehead, AN. *Concept of Nature*, Tarnier Lectures delivered in Trinity College, Cambridge, November 1919, Gutenberg eBook, 16 July 2006.
7. Cantor G. Über unendliche, lineare Punktmannigfaltigkeiten V. *Mathematische Annalen* 21, 545-591; cited in [8].
8. Rosser JB. *Complex Evolutionary Dynamics in Urban-Regional and Ecologi-Economic Systems*, DOI 10.1007/978-1-4419-8828-7, Springer Science +Business Media, LLC 2011.
9. Mandelbrot BB. *The Fractal Geometry of Nature*, W.H. Freeman, San Francisco, 1983.
10. Lorenz E. N. Deterministic non-periodic ow. *J. Atmos Sci.* 1963, **20**, 130-141.
11. Lorenz E. N. *The Essence of Chaos*, University of Washington Press, Seattle, 1993.
12. Ord, GN. Fractal space-time: a geometric analogue of relativistic quantum mechanics. *J. Phys. A: Math. Gen.* 1983, **16**, 1869-84.
13. Feynman RP and Hibbs AR. *Quantum Mechanics and Path Integrals*, McGraw-Hill, New York, 1965.
14. Nottale L. *Fractal Space-Time and Microphysics: Towards a Theory of Scale Relativity*, World Scientific, 1993.
15. Nottale L. *Scale Relativity and Fractal Space-Time, A New Approach in Unifying Relativity and Quantum Mechanics*, Imperial College Press, London, 2011.
16. El Naschie MS. A review of E infinity theory and the mass spectrum of high energy particle physics. *Chaos Solitons & Fractals* 2004, **19**, 209-36.
17. El Naschie MS. The theory of Cantorian spacetime and high energy particle physics (an informal review). *Chaos, Solitons and Fractals* 2009, **41**, 2635-46.
18. Mauldin RD and Williams SC. Random recursive constructions: asymptotic geometric and topological properties. *Trans. Amer. Math. Soc.* 1986, **295**, 325-46.

19. Ho MW. The story of phi part 1. *Science in Society* 2014, **62**, 24-26. www.academia.edu/7718556/The_Story_of_Phi_Part_1_The_Mathematics
20. "There is something about phi, Chapter 9 - Fractals and the golden ratio" Javier Romanach, YouTube, accessed 1 March 2014, www.youtube.com/watch?v=BURjKRfOA9g
21. Ho MW. Watching the daisies grow. *Science in Society* 2014, **62**, 27-29. www.academia.edu/7718580/Story_of_Phi_Part_2_Watching_the_Daisies_Grow
22. Marek-Crnjac L. The Hausdorff Dimension of the Penrose universe. *Phys. Res. Interna* 2011, 874302, 4 pages
23. Connes A. *Noncommutative Geometry*, Paris, 1994, www.alainconnes.org/docs/book94bigpdf.pdf
24. Ho MW. *The Rainbow and the Worm, the Physics of Organisms*, World Scientific, 1993, 2nd edition, 1996, 3rd enlarged edition, 2008, Singapore and London. www.i-sis.org.uk/rnbwwrm.php
25. Schommers W. Space-time and quantum phenomena. In *Quantum Theory and Pictures of Reality* (W. Schommers ed.), pp. 217-77, Springer-Verlag, Berlin, 1989.
26. El Naschie MS. Quantum collapse of wave interference pattern in the two-slit experiment: a set theoretical resolution. *Nonlinear Sci. Lett. A* 2011, **2**, 1-8.
27. El Naschie MS. Topological-geometrical and physical interpretation of the dark energy of the cosmos as a halo energy of the Schrodinger quantum wave. *J. Mod. Phys.* 2013, **4**, 591-6.
28. Ho MW. E infinity spacetime, quantum paradoxes and quantum gravity. *Science in Society* 2014, **62**, 40-43. www.academia.edu/7718725/E-infinity_space_time_quantum_paradoxes_and_quantum_gravity_story_of_phi_part_6
29. "Our universe continually cycles through a series of 'aeons'", *The Daily Galaxy*, 26 September 2011, www.dailygalaxy.com/my_weblog/2011/09/we-can-see-through-the-big-bang-to-the-universe-that-existed-in-the-aeon-before-.html
30. Eugene WC. An introduction to KAM theory. Preprint January 2008, <http://math.bu.edu/people/cew/preprints/introkam.pdf>
31. Ho MW. Golden cycles and organic spacetime. *Science in Society* 2014, **62**, 32-34.
32. Kolmogorov-Arnold-Moser theorem. Wikipedia, 24 January 2014,
33. Effect of noise on the golden-mean quasiperiodicity at the chaos threshold. www.sgtnd.narod.ru/science/noise/2noise/eng/2noise.htm
34. Arnold tongue. Wikipedia, 4 February 2014. http://en.wikipedia.org/wiki/Arnold_tongue
35. Ivankov NY and Kuznetsov SP. Complex periodic orbits, renormalization, and scaling for quasiperiodic golden-mean transition to chaos. *Phys. Rev. E* 2001, **63**, 046210.
36. Lombardi OW and Lombardi MA. The golden mean in the solar system. *The Fibonacci Quarterly* 1984, **22**, 70-75. www.fq.math.ca/22-1.html
37. Phi and the solar system. f Phi 1.618 The Golden Number, 13 May 2013, www.goldennumber.net/solar-system/
38. "Is the solar system stable?" Scott Tremaine, Institute for Advanced Study, Summer 2011, www.ias.edu/about/publications/ias-letter/articles/2011-summer/solar-system-tremaine
39. Sprott JC. Honors: A tribute to Dr Edward Norton Lorenz. *EC Journal* 2008, 55-61, <http://sprott.physics.wisc.edu/lorenz.pdf>
40. Sprott JC. *Strange Attractors: Creating Patterns in Chaos*, M&T Books, New York, 1993.
41. Viswanath D. Symbolic dynamics and periodic orbits of the Lorenz attractor. *Nonlinearity* 2003, **16**, 1035-56.
42. Birman JS and Williams RF. Knotted periodic orbits in dynamical systems 1. Lorenz's equations. *Topology* 1983, **22**, 47-82.
43. Gutzwiller M. Quantum chaos. *Scientific American* January 1992, republished 27 October 2008, www.scientificamerican.com/article/quantum-chaos-subatomic-worlds/
44. Selvam AM. Cantorian fractal space-time fluctuations in turbulent fluid flows and the kinetic theory of gases. *Apeiron* 2002, **9**, 1-20.
45. Kraut DA, Carroll KS and Herschlag D. Challenges in enzyme mechanisms and energetics. *Ann. Rev. Biochem.* 2003, **72**, 517-71.
46. Ho MW. *Living Rainbow H2O*, World Scientific and Imperial College Press, Singapore and London, 2012.
47. Ho MW. Water is the means, medium, and message of life. *Int. J. Design, Nature and Ecodynamics* 2014, **9**, 1-12.
48. Ho MW. Illuminating water and life. *Entropy* 2014, **16**, 4874-91.
49. Ho MW. Circular thermodynamics of organisms and sustainable systems. *Systems* 2013, **1**, 30-49.
50. Glauber RJ. Coherence and quantum detection. In *Quantum Optics* (RJ Glauber ed.), Academic Press, New York, 1969.
51. Metabolic pathways. Sigma Aldrich, accessed 27 October 2014. www.sigmaaldrich.com/content/dam/sigma-aldrich/docs/Sigma/General_Information/metabolic_pathways_poster.pdf
52. Prigogine I. *Time, structure and fluctuations*. Nobel Lecture, 8 December 1977, www.nobelprize.org/

- nobel_prizes/chemistry/laureates/1977/prigogine-lecture.pdf
53. G. Vitiello, Fractals as macroscopic manifestation of squeezed coherent states and brain dynamics. *J. Physics: Conf Ser* 2012, **380**, 012021 (13 pp).
 54. G. Vitiello, Fractals, coherent states and self-similarity induced noncommutative geometry. *Phys. Lett. A* **376**, 2527-2532 (2012).
 55. G. Vitiello, On the isomorphism between dissipative systems, fractal selfsimilarity and electrodynamics. Toward an integrated vision of Nature. *Systems* **2**, 203-216 (2014).
 56. H. O. Peitgen, H. Jürgens and D. Saupe, *Chaos and Fractals. New frontiers of Science*, (Springer-Verlag, Berlin 1986).
 57. A. A. Andronov, A. A. Vitt, S. E. Khaikin, *Theory of Oscillators*, (Dover Publications, INC, N.Y. 1966).
 58. E. Celeghini, M. Rasetti and G. Vitiello, Quantum dissipation. *Ann. Phys.* **215**, 156-170 (1992).
 59. G. 't Hooft, Quantum Gravity as a Dissipative Deterministic System. *Classical and Quantum Gravity* **16**, 3263-3279 (1999);
 60. M. Blasone, P. Jizba and G. Vitiello, Dissipation and quantization. *Phys. Lett. A* **287**, 205-210 (2001).
M. Blasone, E. Celeghini, P. Jizba and G. Vitiello, Quantization, group contraction and zero point energy. *Phys. Lett. A* **310**, 393-399 (2003).
M. Blasone, P. Jizba, F. Scardigli and G. Vitiello, Dissipation and quantization in composite systems. *Phys. Lett. A* **373**, 4106-4112 (2009).
 61. M. Blasone, P. Jizba and G. Vitiello *Quantum Field Theory and its Macroscopic Manifestations*, (Imperial College Press, London 2011).
 62. Ho MW. Quantum world coming series. *Science in Society* 2004, **22**, 4-15.
 63. El Naschie MS. Quantum loops, wild topology and fat Cantor sets in transfinite high-energy physics. *Chaos, Solitons & Fractals* 2002, **13**, 1167-74.
 64. El Naschie MS. Wild topology, hyperbolic geometry and fusion algebra in high-energy physics. *Chaos, Solitons & Fractals* 2002, **13**, 1935-45.
 65. El Naschie MS. On the exact mass spectrum of quarks. *Chaos Solitons & Fractals* 2002, **14**, 369-76.
 66. El Naschie MS. On a class of general theories for high energy particle physics. *Chaos, Solitons & Fractals* 2002, **14**, 649-68.
 67. Marek-Crnjac L. The mass spectrum of high energy elementary particles via El Naschie's \mathcal{E}^∞ golden mean nested oscillators, the Dunkerly-Southwell eigenvalue theorems and KAM. *Chaos Solitons & Fractals* 2003, **18**, 125-33.
 68. Freeman WJ. *Mass Action in the Nervous System*, Academic Press, New York, 1975, 2004.
 69. Freeman WJ. *Neurodynamics, an Exploration of Mesoscopic Brain Dynamics*, Springer- Verlag, 2000.
 70. Freeman WJ. *How Brains make up Their Minds*, Columbia University Press, 2001.
 71. Umezawa H. *Advanced Field Theory: Micro, Macro and Thermal Physics*, American Institute of Physics, New York, 1993.
 72. Vitiello G. Hiroomi Umezawa and quantum field theory. *NeuroQuantology* 2011, **9**, DOI: 10.14704/nq.2011.9.3.450
 73. Freeman WJ. Origin, Structure, and role of background EEG activity. Part 1. Analytic phase. *Clin Neurol.* 2004, **115**, 2077-88.
 74. Freeman WJ. Origin, Structure, and role of background EEG activity. Part 2. Analytic amplitude. *Clin Neurol.* 2004, **115**, 2089-107.
 75. Freeman WJ. Origin, Structure, and role of background EEG activity. Part 3. Neural frame classification. *Clin. Neurol.* 2005, **116**, 1118-29.
 76. Freeman WJ. Phase transitions in the neuropercolation model of neural populations with mixed local and non-local interactions. *Biol. Cybern.* 2005, **92**, 367-79.
 77. Bassett DS, Meyer-Lindenberg A, Achard S, Duke T, Bullmore E. Adaptive reconfiguration of fractal small-world human brain functional networks. *PNAS* 2006, **103**, 19518-23.
 78. Freeman WJ and Burke BC. A neurobiological theory of meaning in perception. Part 4. Multicortical patterns of amplitude modulation in gamma EEG. *Int J. Bifurc. & Chaos* 2003, **13**, 2857-66.
 79. Freeman WJ and Rogers LJ. A neurobiological theory of meaning in perception. Part 5. Multicortical patterns of phase modulation in gamma EEG. *Int. J. Bifurc. & Chaos* 2003, **13**, 2867-87.
 80. Ricciardi LM and Umezawa H. Brain and physics of many-body problems. *Kybernetik* 1967, **4**, 44-48.
 81. Vitiello G. *My Double Unveiled*, John Benjamin Pub. Co., Amsterdam, 2001.
 82. Umezawa H and Vitiello G. *Quantum Mechanics*, Bibliopolis, Naples, 1985.
 83. Vitiello G. Dissipation and memory capacity in the quantum brain model. *Int. J. Mod. Phys.* 1995, **B9**, 973.
 84. Jibu M and Yasue K. *Quantum Brain Dynamics and Consciousness*, John Benjamin, Amsterdam, 1995.
 85. Del Giudice E, Preparata G and Vitiello G. Water as a free electric dipole laser. *Phys. Rev. Lett.* 1988, **61**, 1085-88.
 86. Plenz D. Neuronal avalanches and coherence potentials. *Eur. Phys. J. Special Topics* 2012, **205**, 259-301.
 87. Ho MW. Golden music of the brain. *Science in Society* 2014, 62.
 88. Pletzer B, Kerschbaum H and Kliesch W. When frequencies never synchronize: the golden mean and the resting EEG. *Brain Research* 2010, **1335**, 91-102.

89. Roopun RK, Kramer MA, Carracedo LM, Kaiser M, Davies CH, Traub RD, Kopell NJ and Whittington MA. Temporal interactions between cortical rhythms. *Frontiers in Neuroscience* 2008, doi:10.3389/neuro.01.034.2008

